Numerical Study of Synthetic Jet Actuator Effects in Boundary Layers

Hilton C. de M. Mello
hcmmello@sc.usp.br
University of São Paulo
School of Engineering, São Carlos
13566-590 São Carlos, SP. Brazil

Fernando M. Catalano
catalano@sc.usp.br

Leandro F. de Souza
Member, ABCM
lefraso@icmc.usp.br
University of São Paulo
Mathematics and Computing Sciences Institute
13566-590 São Carlos, SP. Brazil

This work has as a fundamental objective the numerical study of the effects of synthetic jet actuators on the flow of the boundary layer developed on a flat plate and on a hypothetical airfoil. The aim is to obtain computational data to indicate how these effects may be used as a means of flow control, describing the dynamics of the synthetic jet in the presence of external flow. The present paper uses a spatial Direct Numerical Simulation (DNS) to solve the incompressible Navier-Stokes equations, written in vorticity-velocity formulation. The spatial derivatives are discretized with a sixth order compact finite difference scheme. The Poisson equation for the normal velocity component is solved by an iterative Line Successive Over Relaxation Method and uses a multigrid Full Approximation Scheme to accelerate the convergence. The results of simulations with different values of frequency, amplitude and slot length were analyzed through a temporal Fourier analysis. Through this analysis the decision as to which are the better parameters to delay the separation of the boundary layer is examined.
Keywords*: synthetic jet, active flow control, laminar flow transition, delay of separation, Falkner-Skan boundary layer*

Introduction

Several studies demonstrate that flow control can be used to delay the separation of a boundary layer. Experimental work has been done to demonstrate and evaluate drag reduction techniques that have definite possibilities of influencing, for instance, the project of an aircraft. Experiments have demonstrated that, using this technique, it is possible to achieve separation delay of a boundary layer in flows over airfoils. The improvement in the capacity of the boundary layer to overcome an adverse pressure gradient is attributed to the increase of the mixture between the low momentum fluid close to the wall and the high momentum external flow. The successful application of the method increases the lift while maintaining low drag. At low Mach numbers, where high lift for takeoff or landing is required, the boundary layer separation delay allows the increase in payload aircaraft.

Passive flow control does not interact dynamically with the flow. Examples of passive means are slats, flaps and vortex generators. Active flow control acts in a dynamic way with the flow, modifying it. Examples of active flow control are synthetic jet, suction and blowing. Synthetic jet actuators have been used as an active flow control technique. The development of jets with zero net flow mass was the result of several investigations that employed experimental and computational methods, both used in a complementary way. The experimental data provide not only the physical base for the study, but also a database, against which the computational data may be verified. The validated computational model may be used to examine flow details that are hard to analyze experimentally.

The synthetic jet actuator may be considered an attractive device for future use for several reasons. The device is made-up by a cavity with a movable membrane connected to an orifice; it can be manufactured in small dimensions. It is of simple construction and does not depend on micro machining. With the above-mentioned attributes, it is easy to manufacture the actuators and to modify their geometric parameters. Also, they operate with zero net mass flow, that is, they synthesize a jet from the flow field. Thus, no piping system is necessary for the actuator, greatly simplifying the installation.

The membrane oscillation is capable of modifying the flow in the cavity of the synthetic jet actuator and to influence the boundary layer flow. The produced effects depend on the parameters of the jet and orifice. There exists an external floweffect over the flow inside the cavity, however this is not taken into account in the present study.

In the present study a numerical simulation is used to study the effects of a synthetic jet in boundary layers. The synthetic jet is introduced via a slot in the wall. The results are analysed after the variables reach a periodic behaviour. The analyses are carried out by a temporal Fourier of the results near the outflow of the domain. The results show that an increase in the wall normal derivative of the streamwise velocity component ($\partial u/\partial y$) can be reached with proper jet parameters, postponing the separation of the flow.

The present work is divided as follows: the next section presents a description of the first works conducted with synthetic jet actuators, as well as the evolution of these devices for active flow control and their advantages in relation to other control techniques; in the subsequent section, the adopted numerical method is described; in the results and discussion section are presented the numerical results of the effects produced by the synthetic jet on a flat plate boundary layer and on a hypothetical airfoil boundary layer (Falkner-Skan boundary layer). The last section presents the conclusions obtained from the numerical simulations.

Nomenclature

A = *amplitude, dimensionless*
b = *oscillation frequency, dimensionless*
d = *slot length, dimensionless*
d_c = *cavity diameter, m*
d_o = *orifice diameter, m*
$\bar{d}$ = *slot length, mm*
F^+ = *reduced frequency, dimensionless*
f = *dimensionless stream function*
f^* = *nominal oscillation frequency, Hz*
h_c = *cavity height, m*
h_o = *orifice height, m*
L = *reference length, m*
i = *streamwise grid point index, dimensionless*
Re = *Reynolds number of the air flow, dimensionless*
t = *time, dimensionless*
$\bar{t}$ = *time, s*
U_∞ = *free stream velocity, m/s*
u = *streamwise velocity component, dimensionless*

Paper accepted October, 2006. Technical Editor: Aristeu da Silveira Neto.

$\bar{u}$ = *streamwise velocity component, m/s*
v = *normal velocity component, dimensionless*
$\bar{v}$ = *normal velocity component, m/s*
x = *spatial coordinate in streamwise direction, m*
$\bar{x}$ = *spatial coordinate in streamwise direction, dimensionless*
x_{te} = *distance from actuator to trailing edge, m*
Y = *membrane deflection, m*
y = *spatial coordinate in normal direction, m*
$\bar{y}$ = *spatial coordinate in normal direction, dimensionless*

Greek Symbols

α = airfoil angle of attack, deg
β = parameter of Falkner-Skan equation, dimensionless
ε = parameter of the blowing-suction region, dimensionless
η = dimensionless coordinate
μ = fluid dynamic viscosity, Kg/ms
ρ = specific mass, Kg/m^3
Ω = vorticity, dimensionless
ω = actuator frequency, dimensionless

Subscripts

c relative to the airfoil chord
∞ free stream conditions
1 relative to the initial point of the slot
2 relative to the final point of the slot

Flow Control with a Synthetic Jet Actuator

One of the first studies using synthetic jet actuators in active flow control was made by Smith and Glezer (1994). The device used, when applied in a flow field, produced unique effects that are not reproducible with suction or blowing in a fixed or pulsed process. Synthetic jets with low Reynolds numbers have been studied extensively, both experimentally and numerically.

The synthetic jet appeared as one of the most useful devices of active flow control, with several potential applications. Some of the applications seen in studies include: transition control (Lorkowski et al., 1997); separation delay (Sinha and Pal, 1993); effective vortex control (Roos, 1997); vectored propulsion of jet motors (Smith and Glezer, 1997); mixture upgrading for active control of separation (Davis and Glezer, 1999); and turbulence in boundary layers (Crook et al., 1999). At the present time, of all the flow control actuators being studied, most of them are synthetic jets actuators.

The use of acoustic excitement for separation control was investigated by Huang et al. (1987) and Hsiao et al. (1990). They used an acoustically driven cavity, within a NACA 63_3-018 airfoil, to excite the boundary layer through a small rectangular slot, located close to the airfoil leading edge. Both studies used the sound pressure level above the orifice to characterize the control input. Whereas the work of Huang et al. (1987) was limited to the airfoil shedding frequency, that is, dimensionless frequency $F^+ \cong 1$ (nominal frequency $f^* \cong 110$ Hz), Hsiao et al. (1990) investigated the jet actuators performance for a range of frequencies up to $f^* \cong 5000$ Hz. These works reached an increment of 40% in the lift coefficient at post-stall angles of attack. Bremhorst and Hollis (1990) accomplished a study with flow control being executed through the use of steady and pulsed jets.

Numerical simulations published recently by Wu *et al*. (1998) show that the introduction of oscillatory excitement in a separated boundary layer, at low Reynolds and Mach numbers, can increase significantly the post-stall lift at excitement frequencies that are 0.3 to 4 times the natural frequency of vortex shedding. That is, in this case $F^+ = 0.4$ ($F^+ \equiv f x_{te}/U_\infty$). By using frequencies that are at least twice the shedding frequency (which corresponds in our definition to $F^+ \approx 0.8$) the improvement in lift is accompanied by a significant reduction in drag. In a later work of Chang *et al*. (1992), with a two-dimensional airfoil (NACA 63_3-018), the orifice velocity was calibrated so the authors could demonstrate the effect of the frequency on the separation control at low poststall angles of attack ($15° < \alpha < 20°$) and at an airfoil chord based Reynolds number of $3x10^5$.

Rizzetta *et al*. (1998) included the cavity flow as part of direct numerical simulations of synthetic jet flow and verified that significant differences arise when the cavity flow is neglected. Udaykumar et al. (1999) developed an unsteady moving solver that allows simulation of unsteady viscous incompressible flows with complex immersed moving boundaries on Cartesian grids. The fundamental advantage of this method is that the whole geometry of the synthetic jet with an oscillating membrane is modeled in a fixed Cartesian mesh. Carpenter et al. (1998) employed a velocity-vorticity method to compute the entire flow. The interaction of synthetic jets with a transverse flow can lead to a modification in the aerodynamic shape of blunt bodies and, in that way, control flow separation. This idea was used by Amitay et al. (1997) on a flow over a circular cylinder. Depending on the azimuthal position of the jets, a new aerodynamic profile of the cylinder was apparent and an asymmetric pressure distribution developed around the cylinder.

The sensitivity of the attached flow to the excitation frequency is also demonstrated in the numerical simulation of Donovan et al. (1998). They investigated flow reattachment over a NACA 0012 airfoil using time-harmonic zero mass flux blowing. Those simulations showed a 20% post-stall increase in lift at α=22°.

Synthetic jets have recently been used for several applications of flow control, including controlling transition, delaying separation and effecting vortex control. However, there have been just a few experimental investigations of their operations. Smith and Glezer (1998) noticed that synthetic jets, generated using rectangular plane slots, exhibit a standing vortex near the exit of the slot. This was explained as being due to turbulent dissipation of the vortex cores. The same effect can be verified in works with acoustic streaming, where this phenomenon appears when sound waves induce unidirectional flow. It typically has a very weak effect unless the sound waves are attenuated in some way. For synthetic jets, the attenuation is provided by the slot and also through viscous dissipation. However, the synthetic jet flow is not just induced by the acoustic streaming, but also by the movement of a membrane.

In the work of Rathnasingham and Breuer (1997), two-dimensional simulation of an unsteady flow through the orifice introduces viscous effects that are characterized by the Stokes parameter based on the orifice diameter. Rao et al. (2000) performed two-dimensional simulations of synthetic jet, and showed that the optimized configuration depends on a parameter based on the average momentum added to the flow over an operation of the oscillatory jet.

Kral et al. (1997) performed numerical simulations of synthetic jet flow neglecting the cavity, with good agreement with the results of Smith and Glezer (1997), for which the flow was assumed to be completely turbulent. Cain et al. (1998) extended this work including the compressibility effects. They verified that as the jet Mach number increased, the acoustic waves induced by the jet became much stronger.

Today there are efforts to study numerically the flow field within the actuator cavity, as well as of its exterior, by obtaining solutions to the unsteady compressible Navier-Stokes equations (Rizzetta et al., 1998). This is accomplished for the interior flow by the use of an overset deforming zonal grid system. The solutions for the external jet flow field are considered in both two and three spatial dimensions using a high order implicit compact finite difference scheme. In the work of Pes et al. (2002), two-dimensional

synthetic jet unsteadiness is modeled, and simulations are performed to characterize the behavior of an isolated jet with different frequency and amplitude of piston oscillations. Mallinson et al. (2001) investigated the flow generated by a synthetic jet actuator with a circular orifice using an unsteady incompressible two-dimensional numerical simulations.

In the present study a two-dimensional numerical simulation is used to study the effects of a synthetic jet in boundary layers using a Direct Numerical Simulation (DNS) to solve the incompressible Navier-Stokes equations, written in vorticity-velocity formulation. The results indicate that a combination of parameters should be used to delay the fluid flow separation.

Numerical Method

The parameters analyzed in the present two-dimensional study are the amplitude and frequency of the jet, and the slot length, where the jet is introduced.

The following non-dimensionalization was used:

$$x = \frac{\bar{x}}{\bar{L}},\ y = \frac{\bar{y}}{\bar{L}},\ u = \frac{\bar{u}}{\bar{U}_\infty},\ v = \frac{\bar{v}}{\bar{U}_\infty} \tag{1}$$

$$t = t\frac{\bar{U}_\infty}{\bar{L}},\ Re = \frac{\rho \bar{U}_\infty \bar{L}}{\mu},\ \omega = \frac{2\pi f^* \bar{L}}{U_\infty} \tag{2}$$

where x and y are the spatial coordinates in the streamwise and wall normal direction, respectively; u and v are the velocity components in x and y direction, respectively; t is the nondimensional time, and the adopted dimensional parameters were: ρ = 1.2 Kg/m^3, L = 0.05 m, U_∞ = 30 m/s and μ = 1.8 x 10^{-5} Kg/ms. The resulting Reynolds number is Re = 1x 10^5.

The vorticity denoted by Ω, is given by:

$$\Omega = \frac{\partial u}{\partial y} - \frac{\partial v}{\partial x} \tag{3}$$

The vorticity-velocity formulation was adopted in the numeric simulations. Adopting vorticity as being the negative of the rotational of the velocity, equation (3), the vorticity transport equation can be obtained:

$$\frac{\partial \Omega}{\partial t} = -\frac{\partial u\Omega}{\partial x} - \frac{\partial v\Omega}{\partial y} + \frac{1}{Re}\left(\frac{\partial^2 \Omega}{\partial x^2} + \frac{\partial^2 \Omega}{\partial y^2}\right) \tag{4}$$

The continuity equation for the incompressible two-dimensional flow is:

$$\frac{\partial u}{\partial x} + \frac{\partial v}{\partial y} = 0 \tag{5}$$

From the vorticity equation (4) and the continuity equation (5) a Poisson-type equation for the normal velocity component can be derived:

$$\frac{\partial^2 v}{\partial x^2} + \frac{\partial^2 v}{\partial y^2} = -\frac{\partial \Omega}{\partial x} \tag{6}$$

Time integration was done with a fourth order Runge-Kutta scheme (Ferziger and Peric, 1997). The spatial derivatives were discretized using compact finite differences. A 6th order scheme is used for the interior points and a 5th order scheme is used at the boundaries. The details of the discretization scheme can be found in Souza et al (2005).

The unsteady computation starts from a steady state laminar solution. In the present study two different base flows were adopted: a Blasius solution, as a laminar boundary layer developed in a flat plate; and a Falkner-Skan solution as a laminar boundary layer developed in a hypothetical airfoil. The Falkner-Skan solution was obtained for an adverse pressure gradient region, where the boundary layer is susceptible to separation. The Falkner-Skan formula is:

$$f''' + \frac{f.f''}{(2-\beta)} + \beta\frac{1-f'^2}{2-\beta} = 0 \tag{7}$$

The function f denotes the dimensionless stream function. The function $f(\eta)$ depends on the variable η, where the dimensionless coordinate η is:

$$\eta = y\sqrt{\frac{\rho U_\infty}{\mu x}} \tag{8}$$

The hypothetical airfoil was obtained by using β = -0.15x. The Blasius formula is the same, using β = 0. Figure 1 shows the downstream development of the shape factor H_{12} of the Blasius and the hypothetical airfoil boundary in Stemmer (2001).

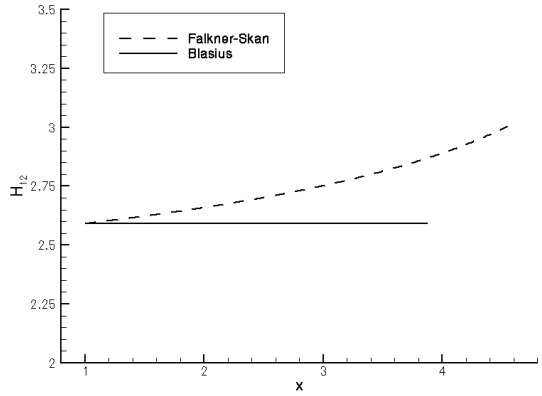

Figure 1. Downstream development of the shape factor for the two base flows used in the simulations.

To simulate the propagation of the synthetic jet in a boundary layer, we must introduce the jet in the computational field. To do that it is necessary to change the boundary conditions at the wall. The jet may be introduced at the wall, through a slot with blowing and suction at a specified frequency. The adopted method consists of introducing a slot at the wall going from grid point i_1 to i_2. The function used for the normal perturbation velocity v is:

$$\begin{cases} v(x,0,t) = g(x)_i\, A \sin \omega t & \text{for} \quad i_1 \le i \le i_2 \\ v(x,0,t) = 0 & \text{for} \quad i < i_1 \quad \text{and} \quad i > i_2 \end{cases} \tag{9}$$

A is real constant which adjusts the amplitude of the synthetic jet. b is the dimensionless frequency. The function $g(x)_i$ adopted here is a function:

$$g(x)_i = sin^3(\varepsilon) \tag{10}$$

where:

$$\varepsilon = \frac{i_2 - i}{i_2 - i_1} \text{ for } i_1 \le i \le i_2 \qquad (11)$$

This function was chosen by comparing the jet profile with experimental results. Now we have a region at the wall where the normal velocity component is different from zero. This v velocity distribution determines the vorticity distribution on the wall through equation (6). A buffer domain was implemented, located near the outflow boundary in order to avoid reflections that could come from this boundary. The code used in the present study was validated beforehand in Direct Numerical Simulations of spatially disturbances propagation, the validation of the code is shown in Souza et al. (2005).

Results and Discussion

The results of simulations with different jet frequency values, amplitude and slot lengths were inspected through a temporal Fourier analysis. Through this analysis it was examined which was the best condition to delay separation of the boundary layer. The total number of points in the streamwise and wall normal direction used in the simulations, on a flat plate boundary layer (Blasius boundary layer), were 257 and 97, respectively; and in the simulations on a hypothetical airfoil boundary layer (Falkner-Skan boundary layer), were 321 and 161, respectively. The dimensionless distance between two consecutive points in the streamwise and wall normal directions were 0.01125 and 0.001, respectively.

Figure 2 shows the computational domain. In the x direction the domain extends from $x_0 = 1$ up to $x_{max} = 3.1375$ in the simulations with the Blasius profile and $x_{max} = 3.7$ in the simulations with the hypothetical airfoil (Falkner-Skan profile). The synthetic jet is introduced between x_1 and x_2. The area between x_3 and x_4 corresponds the relaminarization area, where the oscillations are damped to zero. In the y direction the domain varies from 0 up to y_{max}.

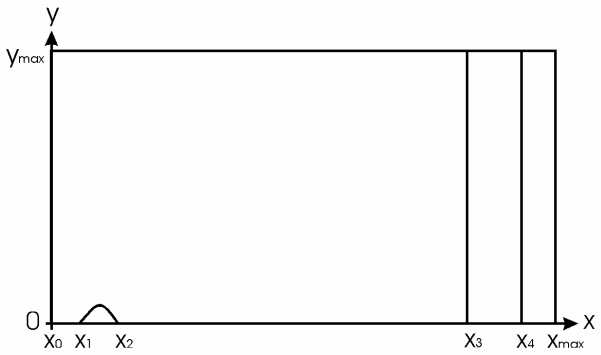

Figure 2. Domain used in the simulations of the boundary layer on a flat plate and on a hypothetical airfoil.

The dimensionless time step used was 0.00393 for a CFL number of 0.35. Fourier temporal analysis of the flow interacting with a synthetic jet was done in the position $x = 3.1375$, in the case of flat plate boundary layer; and $x = 3.7$, in the case of hypothetical airfoil boundary layer. The difference between the base flow and the distorted flow gives an idea of how the synthetic jet is changing the boundary layer profile.

The dimensionless slot lengths of the simulations, $d = 0.09$, 0.135 and 0.225, correspond to the nominal values $\bar{d} = 4.5$, 6.75 and 11.25 mm. The dimensionless frequencies used in the simulations, $\omega = 11$, 13, 15, 17 and 19, correspond to the nominal frequencies $f^* = 1051$, 1242, 1433, 1624 and 1815 Hz.

This section was divided in six subsections: the first, second and third subsections analyze the influence of slot length, frequency and amplitude of the synthetic jet in a flat plate boundary layer. The next three subsections present the same analysis for a hypothetical airfoil boundary layer.

Effect of Slot Length in Simulations of Flow Over a Flat Plate

Figures 3 and 4 show the difference between the derivative of u velocity component in the wall normal direction ($\partial u/\partial y$) of the Blasius profile (base flow) and of the profile of mean velocity u obtained through the Time Fourier analysis in the position $x = 3.1375$. In these figures SJ stands for Synthetic Jet and the distance in y direction was normalized by boundary layer thickness. The influence of the synthetic jet on the flow is clearly shown. In the evaluation of the variation of the dimensions of the slot of the actuator of synthetic jet, simulations show that the largest dimension for the slot of the actuator, $d = 0.225$, provided, in a larger number of cases, a larger increase in $\partial u/\partial y$.

Figure 3 shows the results of the first case, where the size of the slot is varied. The jet pulse amplitude was fixed at $A = 2$. The dimensionless frequency also remained constant corresponding to the value $\omega = 15$. For all the dimensions of slot used, an increase in $\partial u/\partial y$ can be observed in Figure 3 in the region close to the wall, and in the case of the dimension $d = 0.225$, a relatively larger increase in $\partial u/\partial y$ occurs.

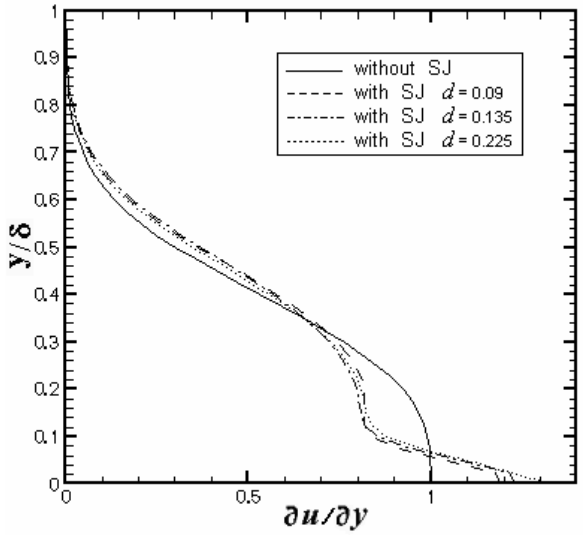

Figure 3. Temporal Fourier analysis with variation of the length slot for $A = 2$ and $\omega = 15$.

In the second case, shown by Figure 4, the same parameters of the first case were used, but the amplitude was increased to the value $A = 4$ and the dimensionless frequency was decreased to value $\omega = 11$. In relation to the $\partial u/\partial y$ variation, it can be observed in Figure 4 that all the dimensions of the slot provide a $\partial u/\partial y$ increase, and this is larger for $d = 0.225$, this result was the best for delaying separation.

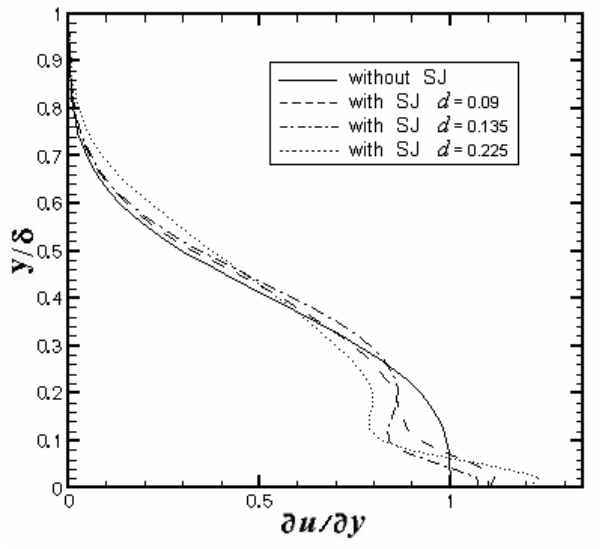

Figure 4. Temporal Fourier analysis with variation of the length slot for A = 4 and ω = 11.

Effect of Frequency in Simulations of Flow Over a Flat Plate

The influence of the oscillation frequency of synthesized flow is analyzed in Figures 5 and 6. In the simulations corresponding to Figure 5, five different values of dimensionless frequency were adopted, corresponding to ω = 11, 13, 15, 17 and 19. In these simulations the size of the slot remained constant with d = 0.225.

The amplitude was fixed at A = 2. It may be observed in Figure 5 that for ω = 11, 13, 15 and 17, these frequencies provide an increase in $\partial u/\partial y$, and for ω = 19, a decrease in $\partial u/\partial y$ occurs in the area close to the wall. In the simulations of the flow on the flat plate, the dimensionless frequency ω = 15, supplied in all the cases, a larger increase in $\partial u/\partial y$.

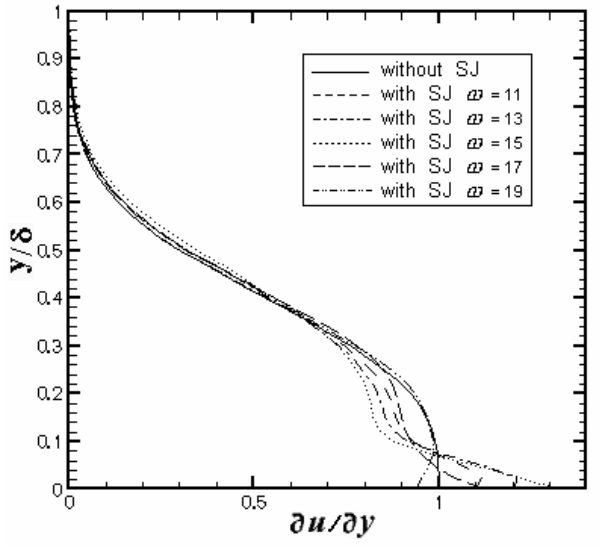

Figure 5. Temporal Fourier analysis with variation of oscillation frequency for A = 2 and d = 0.225.

For the results in Figure 6, the same values of ω were adopted, but the amplitude was fixed at A = 3 and the slot length changed to the value d = 0.135. In the $\partial u/\partial y$ variation, it can be observed in Figure 6 that for ω = 13 and ω = 15, these frequencies provide a larger increase in $\partial u/\partial y$, and for ω = 17 a decrease in $\partial u/\partial y$ occurs showing that a reduction of drag can be obtained with these parameters.

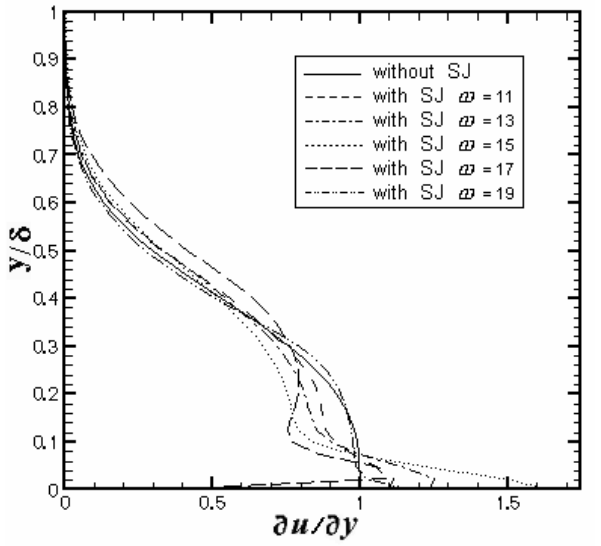

Figure 6. Temporal Fourier analysis with variation of oscillation frequency for A = 3 and d = 0.135.

Effect of Amplitude in Simulations of Flow Over a Flat Plate

The influence of the synthesized flow amplitude was analyzed and the results are shown in Figures 7 and 8. In these simulations four different values for the amplitude were adopted, corresponding to the value A = 2, 3, 4 and 5.

Figure 7 shows the results obtained for the dimensionless frequency ω = 11. The slot length remained fixed with d = 0.135. Figure 7 shows that with relation to the $\partial u/\partial y$ variation, it may be observed that all of the oscillation amplitudes provide a $\partial u/\partial y$ increase, and this increase is relatively larger for A = 5 in the area close to the wall.

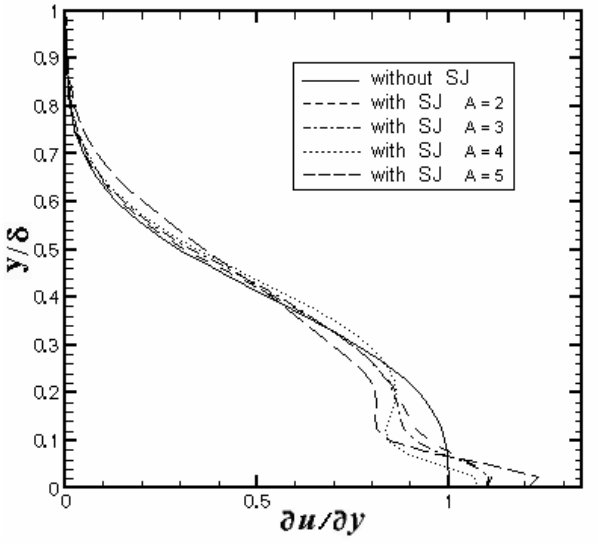

Figure 7. Temporal Fourier analysis with variation of oscillation amplitude for ω = 11 and d = 0.135.

In Figure 8, the dimensionless frequency was fixed at $\omega = 17$ and the slot length changed to the value $d = 0.225$. With reference to $\partial u/\partial y$ variation, Figure 8 shows that for $A = 5$ and $A = 4$ occurs a larger increase of $\partial u/\partial y$ and for $A = 3$ a decrease in $\partial u/\partial y$ it can be observed in the area close to the wall.

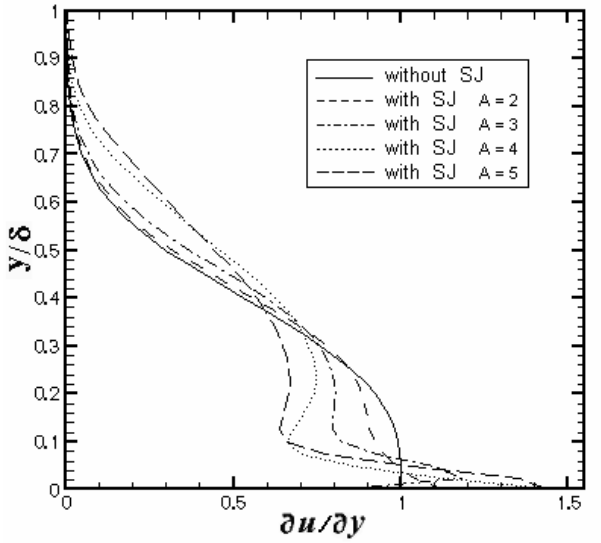

Figure 8. Temporal Fourier analysis with variation of oscillation amplitude for $\omega = 17$ and $d = 0.225$.

Effect of Slot Length in Simulations of Flow Over the Hypothetical Airfoil

The next results were carried out with a Falkner-Skan solution in an adverse pressure region given a hypothetical airfoil boundary layer, in the position $x = 3.7$. In the first case, corresponding to Figure 9, an analysis of the influence of size of the slot was carried out. Three different values were used for $d = 0.09$, 0.135 and 0.225. The amplitude was fixed at $A = 5$ and the dimensionless frequency was fixed at $\omega = 11$.

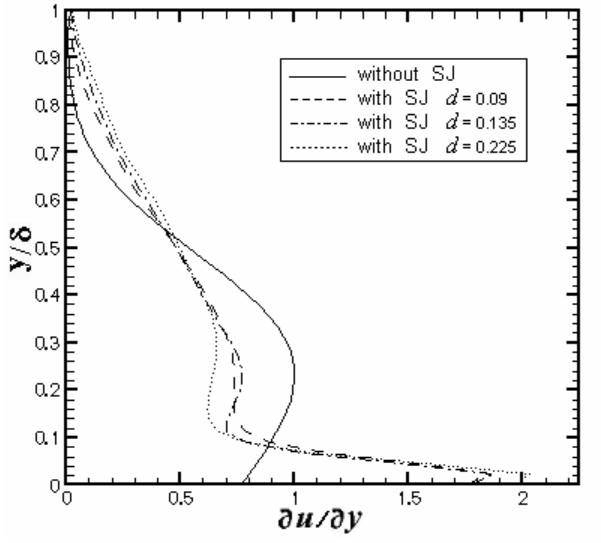

Figure 9. Temporal Fourier analysis with variation of the length slot for $A = 5$ and $\omega = 11$.

Figure 9 shows that in relation to the $\partial u/\partial y$ variation, it can be observed that all the dimensions of the slot provide a $\partial u/\partial y$ increase in relation to the profile of the flow without the presence of the synthetic jet, and this is relatively larger for $d = 0.225$.

Figure 10 shows results for the same values of d, but the value of amplitude $A = 4$ was adopted for the oscillation amplitude and the frequency is maintained constant with $\omega = 11$. In relation to the $\partial u/\partial y$ variation, in the Figure 10 it can be observed that all the slot length provide a $\partial u/\partial y$ increase, being relatively lesser for $d = 0.135$.

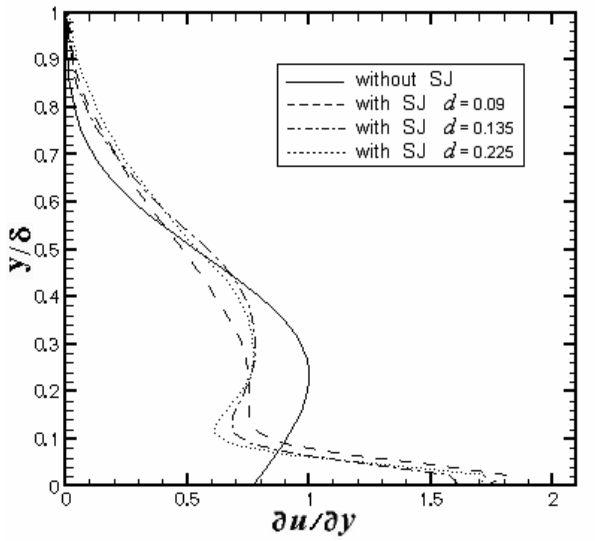

Figure 10. Temporal Fourier analysis with variation of the length slot for $A = 4$ and $\omega = 11$.

Effect of Frequency in Simulations of Flow Over the Hypothetical Airfoil

The influence of the oscillation frequency of synthesized flow is analyzed in Figures 11 and 12. In the simulations corresponding to Figure 11, five different values of dimensionless frequency were adopted, corresponding to $\omega = 11$, 13, 15, 17 and 19.

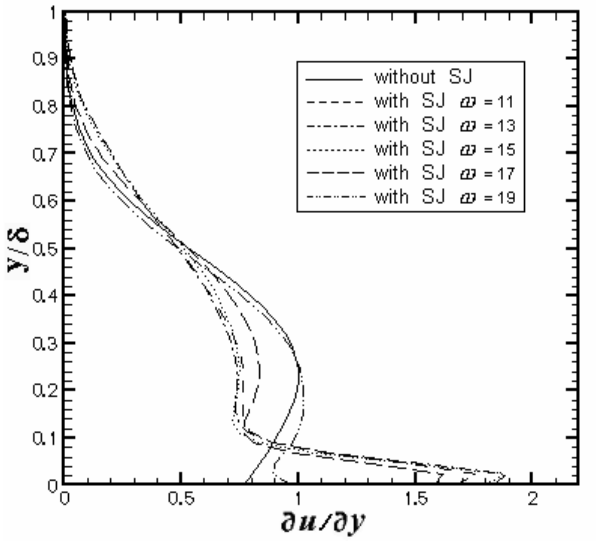

Figure 11. Temporal Fourier analysis with variation of oscillation frequency for $A = 2$ and $d = 0.225$.

The size of the slot was fixed at d = 0.225. For the dimensionless amplitude was attributed the value A = 2. In relation to the $\partial u/\partial y$ variation, Figure 11 shows that for ω = 11, 13, 15 and 17, a significant increase of $\partial u/\partial y$ is obtained, more than the double in relation to the profile without the synthetic jet, and for ω = 19 a smaller increase of $\partial u/\partial y$ occurs in the area close to the wall.

In Figure 12, the same variation of the dimensionless frequency is applied. The value A = 3 is adopted for the oscillation amplitude in the five frequencies analyzed in the simulations. The slot dimension is maintained constant with the value d = 0.09. In relation to the $\partial u/\partial y$ variation, Figure 12 shows that all the dimensionless frequencies provide an increase in $\partial u/\partial y$, presenting more than the double of the value in relation to the flow profile without the synthetic jet.

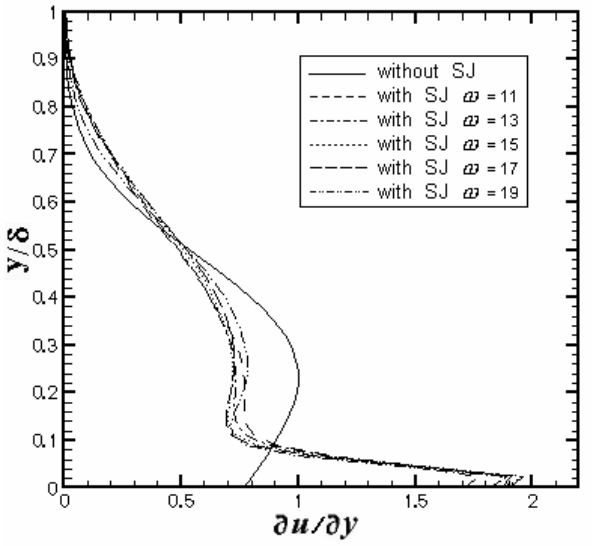

Figure 12. Temporal Fourier analysis with variation of oscillation frequency for A = 3 and d = 0.09.

Effect of Amplitude in Simulations of Flow Over the Hypothetical Airfoil

The influence of the oscillation amplitude of the synthesized flow is analyzed in Figures 13 and 14. In the simulations performed for the flow over the surface of the hypothetical airfoil, the presented results are closer for the four oscillation amplitudes tested. In the simulations of the flow on the surface of the airfoil, the oscillation amplitude of the actuator A = 5, causes a higher increase in $\partial u/\partial y$ in all the tested cases. The results for amplitudes A = 3 and A = 4, are close to those obtained with the larger oscillation amplitude A = 5.

The results shown in Figure 13, four different values of amplitude were adopted, corresponding to A = 2, 3, 4 and 5. The size of the slot was fixed at d = 0.225. For the dimensionless frequency was attributed the value ω = 17. In this case, the largest increase in $\partial u/\partial y$ occurs for amplitude A = 5. Figure 13 shows that with reference to $\partial u/\partial y$ variation, it is observed that all the dimensionless frequencies provide more than the double of $\partial u/\partial y$ increase in relation to the flow profile without the synthetic jet, and is relatively lesser for amplitude A = 2.

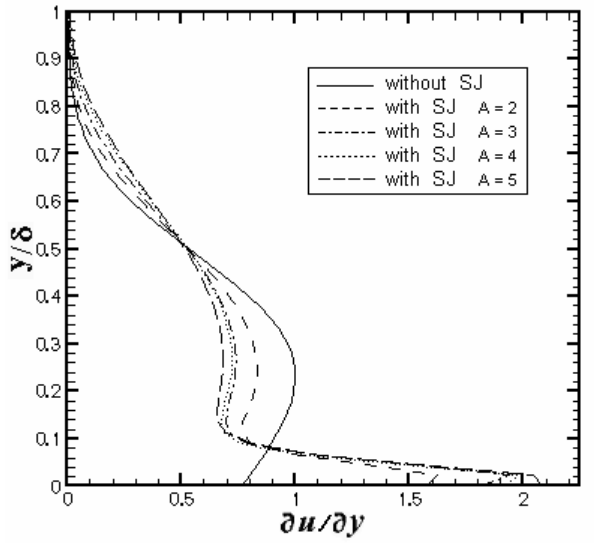

Figure 13. Temporal Fourier analysis with variation of oscillation amplitude for ω = 17 and d = 0.225.

In Figure 14, the same variation of the amplitude is applied. The value ω = 11 was adopted for the dimensionless frequency and the size of the slot was d = 0.135. For this case the largest increment in $\partial u/\partial y$ occurs for the values of amplitude A = 3, 4 and 5. Figure 14 shows that all the oscillation amplitudes provide an $\partial u/\partial y$ increase, and this increase is relatively lesser for A = 4 in the area close to the wall.

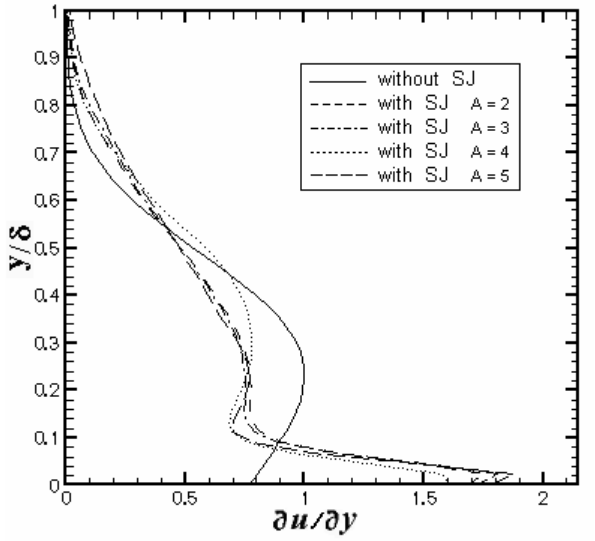

Figure 14. Temporal Fourier analysis with variation of oscillation amplitude for ω = 11 and d = 0.135.

Conclusions

In the present work a numerical study of the synthetic jet influence in Blasius and Falkner-Skan boundary layers were performed. The effect of variation of different parameters was analyzed in the simulations. The simulations results with different frequency, amplitude and slot length values were inspected through a temporal Fourier analysis. Through this analysis the best condition to delay separation of the boundary layer in each test case was examined. Numerical simulations results showed that the introduction of the synthetic jet contributed to an increase of *du/dy*

near the wall. The flow oscillations introduced by the synthetic jet induced an acceleration of the flow near the surface of the flat plate. In some cases, for certain combinations of frequency, slot length and oscillation amplitude, larger increments of du/dy were observed. The main conclusion in this work is that in relation to the $\partial u/\partial y$ variation, the results show that the performance of the synthetic jet provided a $\partial u/\partial y$ increase, presenting more than the double of the value in relation to the flow profile without the synthetic jet. The flow oscillations introduced by the synthetic jet caused an acceleration of the flow close to the surface of the flat plate. The results of $\partial u/\partial y$ increase in the case of the airfoil are larger in relation to the results obtained in the flow simulations on a flat plate. Although the study results show that inflections are introduced in the streamwise velocity component, making the flow more susceptible to transition from laminar to turbulence state, the idea of the synthetic jet is to avoid separation, increasing du/dy near the wall.

References

Amitay, M., Honohan, A., Trautman, M. and Glezer, A., 1997, "Modification of the Aerodynamic Characteristics of Bluff Bodies Using Fluidic Actuators", AIAA Paper 97-2004, Jun.

Bremhorst, K. and Hollis, P.G., 1990, "Velocity Field of an Axisymmetric Pulsed, Subsonic Air Jet", AIM J, 28, pp 2,043-2,049.

Cain, A. B., Kral, L. D., Donovan, J. F. and Smith, T. D., 1998, "Numerical Simulation of Compressible Synthetic Jet Flows", AIAA paper 98-0084.

Carpenter, P. W., Davies, C. and Lockerby, D. A., 1998, "A Novel Velocity Vorticity Method for Simulating the Effects of MEMS Actuators on Boundary Layers", 5th Asian CFD Conference, Bangalore, India, 7-11 December.

Crook, A., Sadri, A. M. and Wood, N. J., 1999, "The Development and Implementation of Synthetic Jets for the Control of Separated Flow", AIAA Paper 99-3176, July.

Davis, S. A. and Glezer, A., 1999, "Mixing Control of Fuel Jets Using Synthetic Jet Technology: Velocity Field Measurements", AIAA paper 99-0447.

Donovan, J. F., Kral, L. D. and Cary, A. W., 1998. "Active Flow Control Applied to an Airfoil", AIAA Paper 98–0210.

Ferziger, J. H. and Peric, M., 1997, "Computational Methods for Fluid Dynamics", Springer-Verlag (Berlin) Heidelberg (New York).

Hsiao, F. B., Liu, C. F. and Shyu, J. Y., 1990, "Control of Wall Separated Flow by Internal Acoustic Excitation", AIAA Journal, Vol. 28, No. 8.

Huang, L. S., Maestrello, L. and Bryant, T. D., 1987, "Separation Control over an Airfoil at High Angles of Attack by Sound Emanating from the Surface", AIAA Paper 87-1261, March.

Kral, L. D., Donovan, J. F., Cain, A. B. and Cary, A. W., 1997, "Numerical Simulations of Synthetic Jet Actuators", AIAA paper 97-1984.

Lorkowski, T., Rathnasingham, R. and Breuer, K. S., 1997, "Small Scale Forcing of a Turbulent Boundary Layer", AIAA paper 97-1792.

Mallinson, S. G., Reizes, J. A., Hong, G., 2001, "An experimental and Numerical study of Synthetic Jet Flow", The Aeronautical Journal Paper, n. 2533, pp. 41-49.

Pes, M., Lukovic, B., Orkwis, P. D., Turner, M. G., 2002, "Modeling of Two Dimensional Synthetic Jet Unsteadiness Using Neural Network Based Deterministic Source Terms", AIAA Paper, 2002-2860.

Rao, P. P., Gilarranz, J. L., Ko, J., Strganac, T., Rediniotis, O. K., 2000, "Flow Separation Control Via Synthetic Jet Actuation", AIAA Paper, 2000-0407.

Rathnasingham, R., Breuer, K. S., 1997, "Coupled Fluid Structural Characteristics of Actuators for Fluid Control", AIAA Journal, Vol. 35, pp. 832-837.

Rizzetta, D. P., Visbal, M. R. and Stanek, M. J., 1998, "Numerical Investigation of Synthetic Jet Flow Fields", AIAA paper 98-2910.

Roos, F. W., 1997, "Synthetic Jet Micro-blowing for Vortex Asymmetry Management on a Hemisphere Cylinder Forebody", AIAA paper 97-1973.

Seifert, A. and Pack, L.G., 1998 "Oscillatory Control of Separation at High Reynolds Numbers", AIAA paper 98-0214.

Sinha, S. K. and Pal, D., 1993, "On the Differences Between the Effect of Acoustic Perturbation and Unsteady Bleed in Controlling Flow Separation Over a Circular Cylinder", SAE Tech Paper 932573.

Smith, B. L. and Glezer, A., 1994, "Vectoring of a High Aspect Ratio Rectangular Air Jet Using a Zero Net Mass Flux Control Jet", American Physics Society, Vol. 39.

Smith, B. L. and Glezer, A., 1997, "Vectoring and Small Scale Motions Effected in Free Shear Flows Using Synthetic Jet Actuators", AIAA Paper 97-0213, January.

Smith, B. L. and Glezer, A., 1998, "The Formation and Evolution of Synthetic Jets", Physics Fluids, No. 10, pp 2.281-2.297.

Souza, L. F., Mendonça, M. T. and Medeiros, M. A. F., 2005, "The advantages of using high-order finite differences schemes in laminar-turbulen transition studies", Int. Journal for Numerical Methods in Fluids, Vol. 48. pp 565-592.

Stemmer, C., 2001, " Direct Numerical Simulation of Harmonic Point Source Disturbances in a Airfoil Boundary Layer with Adverse Pressure Gradient", PHD Thesis, IAG Universität Sttutgart.

Udaykumar, H. S., Mittal, R. and Shyy, W., 1999, "Solid Liquid Phase Front Computations in the Sharp Interface Limit on Fixed Grids", J. Comput. Phys. Vol. 18, pp. 535-574.

Wu, J.Z., Lu, X.Y., Denny, A.G, Fan, M. and Wu, J.M., 1998, "Post-Stall Flow Control on an Airfoil by Local Unsteady Forcing", Journal of Fluid Mechanics, Vol. 371, pp. 21-58.